Hermaphroditic liquid-crystal microlens

Hongwen Ren, Janet R. Wu, Yun-Hsing Fan, Yi-Hsin Lin, and Shin-Tson Wu

College of Optics and Photonics, University of Central Florida, Orlando, Florida 32816

Received September 13, 2004

We demonstrate a flat microlens that exhibits hermaphroditic focusing properties. When the input polarization is parallel (perpendicular) to the liquid-crystal directors, the lens exhibits a positive (negative) focal length. To select the proper polarization, we could rotate the polarizer (or the lens) mechanically or by use of an electrically controlled twisted nematic liquid-crystal cell. Details of the lens structure and of the device's fabrication and performance are described. © 2005 Optical Society of America

OCIS codes: 230.3270, 350.3950, 160.3710.

Liquid-crystal- (LC-) based microlens arrays have potential applications in optoelectronics, integrated optics, information processing, optical communications, and three-dimensional displays. Various fabrication methods, such as techniques that involve zone patterned structures,[1] holes or hybrid-patterned electrodes,[2–4] surface-relief profiles,[5–9] and inhomogeneous polymer network LCs,[10,11] have been proposed, and the general operation mechanism is based on electric-field-induced gradient refractive indices. Among these approaches, homogeneously aligned LC cells are commonly utilized because of their large refractive-index change. To vary the focal length we apply an external voltage across the LC lens. Because of the electric-field-induced molecular reorientation, the optical path difference between the edges and center of the lens can be tuned.

Most LC lenses are polarization sensitive. When the polarization of the incoming light is parallel to the direction of LC alignment, i.e., is an extraordinary ray, the focal length of the LC lens can be tuned continually within a finite range that depends on the LC's birefringence. However, for an ordinary ray (i.e., polarization of the incident light perpendicular to the LC directors), the focal length of the LC lens does not change with voltage. Both positive and negative lenses can be designed according to need. However, once a lens is designed to have a positive (negative) focal length, it remains positive (negative). Although under some special operating conditions the central part of a positive LC lens can exhibit a negative focusing property,[12] the surrounding part remains positive. This volcano type of LC lens suffers from severe index distortion.

In this Letter we demonstrate a flat LC microlens that exhibits either a positive or a negative focal length, depending on the polarization of the input light. Unlike a conventional LC lens whose focal length is tunable by applied voltage, our hermaphroditic LC microlens changes focal length according to the angle between the polarization axis and the LC directors. For an extraordinary ray, the focal length is positive, whereas for an ordinary ray the focal length becomes negative. By changing the relative angle between the polarization of the incident light and the LC directors, we can vary the focal length of the LC lens. This polarization rotation can be achieved manually or by an electrically controlled 90° twisted nematic (TN) cell.[13]

Figure 1 depicts a side view of the microlens array. This flat lens comprises a plano–convex LC lens and a plano–concave molded polymeric lens (shaded areas). In this study, the LC directors in the plano–convex lens are aligned along the x axis. The ordinary and extraordinary refractive indices (n_o and n_e) lie along the y and x axes, respectively, as indicated in Fig. 1. The plano–concave lens is made from an UV-cured polymer–LC composite upon a polyimide surface whose rubbing direction is along the y axis. Thus its refractive indices are also anisotropic: $n_1 > n_2$. For our lens design we chose material systems that would satisfy the following relationship: $n_e \sim n_1 > n_2 \sim n_o$. When the incident light passes through the convex and concave lenses from the z axis with its polarization at an angle θ with respect to the x axis, the focal length of the microlens can be expressed as

$$f = R/(n_{\mathrm{LC}} - n_{\mathrm{mold}}), \tag{1}$$

where R is the radius of curvature of a lens's surface and n_{LC} and n_{mold} denote the effective refractive indices of the LC and the molded polymeric lenses, respectively. Both n_{LC} and n_{mold} are dependent on θ:

$$n_{\mathrm{LC}} = \frac{n_o n_e}{(n_o^2 \cos^2\theta + n_e^2 \sin^2\theta)^{1/2}}, \tag{2}$$

$$n_{\mathrm{mold}} = \frac{n_1 n_2}{(n_1^2 \cos^2\theta + n_2^2 \sin^2\theta)^{1/2}}. \tag{3}$$

From Eqs. (1)–(3), when $\theta = 0$, the focal length of the lens is $f_1 = R/(n_e - n_2)$. In this case, focal length f_1 is positive. If $\theta = 90°$, the focal length of the lens is $f_2 = R/(n_o - n_1)$. Because $n_o < n_1$, focal length f_2 is negative. When $n_{\mathrm{LC}} \sim n_{\mathrm{mold}}$, the focal length of the lens approaches infinity. Tuning the axis of polarization of the incident light gradually from 0 to 90° changes the focal length from positive to negative.

To fabricate the desired anisotropic polymeric lens with $n_1 > n_2$ as depicted in Fig. 1, we mixed 80 wt.% of RM257 (a diacrylate monomer doped with 1-wt.%

0146-9592/05/040376-03$15.00/0

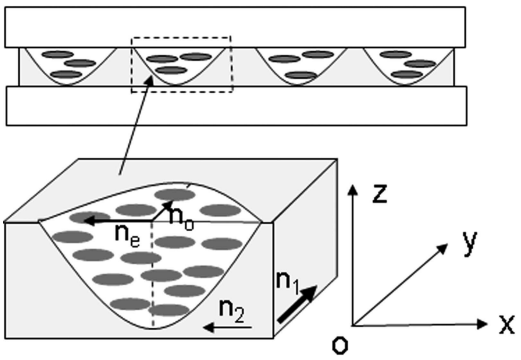

Fig. 1. Side view of hermaphroditic LC microlens arrays: n_1 and n_2 are the refractive indices of the molded microlenses along the y and x axes, respectively, and n_o and n_e are the ordinary and extraordinary refractive indices of the LC material.

photoinitiator IRG184) with 20 wt. % of a Merck nematic LC, TL-205 ($n_o = 1.527$, $n_e = 1.744$). First we coated the LC–monomer mixture onto a bottom glass substrate at ~80 °C. The inner surface of the glass plate was spin coated with a thin (~80-nm) polyimide layer, baked, and then rubbed along the y axis. We then used a glass plano–convex microlens array as a stamper to create concave cavities over the coated mixture. The patterned LC–monomer mixture was cooled to 50 °C and then exposed to UV light with intensity $I = 15$ mW/cm^2 for ~5 min. After UV exposure, the stamper was peeled off and the solidified concave microlens patterns remained on the glass substrate. The strong anchoring energy of the polyimide-coated bottom glass substrate influences the LC–monomer alignment during the UV-induced polymerization process. As a result, an anisotropic polymeric concave lens with $n_1 > n_2$ is achieved.

In the last step, we injected pure LC TL-205 into the molded polymer cavities and sealed them with a top glass substrate. The inner surface of the top glass plate also had a thin rubbed polyimide layer. The rubbing direction are along the x axis, which was orthogonal to that of the bottom glass substrate. The sealed cell was reheated at ~90 °C and then cooled from the injected pure-LC side to room temperature to produce homogeneous LC alignment.

Before filling the LC and putting on the top glass plate we measured the thickness (d) and the radius of curvature (R) of the molded polymeric lens. We found that $d \sim 50$ μm and $R \sim 0.64$ mm. We inspected the anisotropic property of the molded cavity arrays by observing the image of a small object through it, using a polarized optical microscope. As shown in Fig. 2, from the bottom up the incident light passes through a polarizer, a green filter ($\lambda = 546$ nm), an object R, a sample stage, and an eyepiece. First, we adjusted the rubbing direction of the molded cavity arrays to be parallel to the polarizer's transmission axis. By adjusting the distance between the ocular and the sample, we observed multiple reversed images of the object through the cavity arrays, as shown in Fig. 3(a). When the sample on the microscope stage was rotated gradually, the observed images were blurred. When the rubbing direction was perpendicular to the polarizer's axis, the blurriest images were observed, as shown in Fig. 3(b). Moving the sample toward the ocular direction, as shown in Fig. 2(c), caused the images to become clear again, but the sizes of the images had shrunk, as shown in Fig. 3(c). This result implies that each of the molded cavities functions as a microlens and that the microlens exhibits anisotropic focusing properties.

To measure the focal length of the molded concave microlens arrays we initially focused on the microlens's surface and then raised the sample stage until a sharp image was found. The distance that the sample traveled was equal to the sample's focal length. According to the measurement, the focal lengths of the molded concave arrays parallel and perpendicular to the sample's rubbing direction are $f_1 \sim -0.62$ mm and $f_2 \sim -0.76$ mm, respectively. Correspondingly, the refractive indices of n_1 and n_2 were calculated to be 1.66 and 1.54, respectively.

After having characterized the molded polymeric cavity arrays, we injected pure LCs (Merck TL-205) into the cavities, and planar microlens arrays were formed. The imaging properties of the planar microlens arrays were also evaluated by use of the same polarized optical microscope. The setup is similar to that shown in Fig. 2. Figure 4(a) shows LC alignment parallel to the polarizer's axis [Fig. 2(a)]. By adjusting the distance between the ocular and the sample, we observed multiple erected images of the object through the microlens arrays. The images are magnified significantly because each microlens has a positive focus. By rotating the polarization axis of the

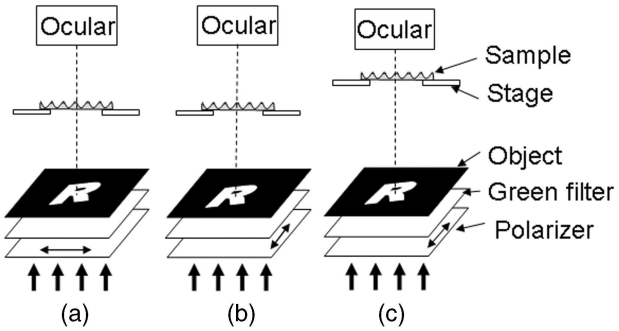

Fig. 2. Experimental setup used for observing the imaging behavior of the molded cavity arrays. The rubbing direction of the molded cavity arrays is (a) parallel, (b) perpendicular, and (c) perpendicular to the polarizer's transmission axis. The position of the sample in Fig. 2(c) is closer to the eyepiece.

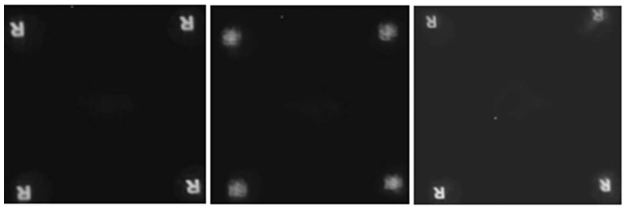

Fig. 3. Imaging properties of the molded cavity arrays: (a), (b), (c) correspond to the setups observed in Figs. 2(a), 2(b), and 2(c), respectively.

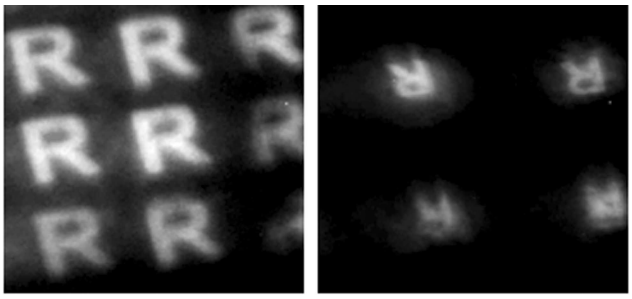

Fig. 4. Imaging properties of the planar LC microlens arrays: (a), (b) images observed that correspond to the setups shown in Figs. 2(a) and 2(c), respectively.

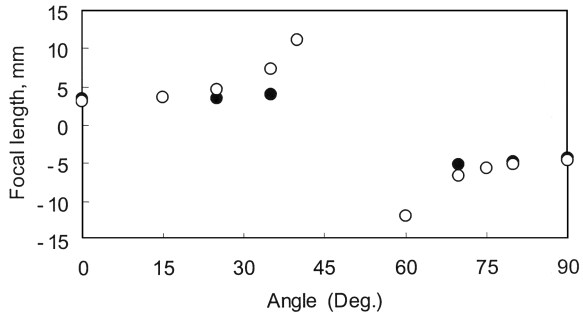

Fig. 5 Angular-dependent focal lengths of the demonstrated microlens arrays. Filled and open circles, measured and calculated results, respectively.

analyzer 90° and moving the sample toward the ocular direction, we observed multiple reversed images, as shown in Fig. 4(b). The size of the image is reduced because each microlens has a negative focus.

The relationship between the rotation angle and the focal length of a microlens was measured with a polarized optical microscope, and the results (filled circles) are plotted in Fig. 5. Here the incident beam is normal to the lens's surface. As the LC alignment is parallel to the polarization of the incident light ($\theta = 0$), the focal length of the lens is positive but short. As θ increases gradually, the focal length increases and then approaches infinity, as indicated by the open circles. When the LC alignment is perpendicular to the polarization of the incident light ($\theta = 90°$), however, the focal length is short and negative. At a smaller angle, the focal length remains negative but increases gradually. When the rotating angle is near 45°, it is difficult to measure the focal length because the focal length is long and the error is relatively large. Using Eqs. (1)–(3), we were able to calculate the rotation-angle-dependent focal length. Results are plotted as open circles in Fig. 5. The measured and calculated results agree fairly well.

Besides manually rotating the polarizer or the LC lens, we can use an electrically switchable 90° TN cell[13] to select the polarization state. The use of a TN cell has to be accompanied with that of a linear polarizer. Let us assume that the polarizer's transmission axis is the y axis. In the voltage-off state, the TN cell rotates the polarization of the incident beam by 90°; i.e., the position of the outgoing light is parallel to the x axis, as shown in Fig. 1, and the lens has a positive focal length. In a high-voltage state, the polarization rotation effect vanishes; thus the output polarization is still on the y axis. Under such a circumstance, the microlens has a negative focal length. The switching time depends on the LC cell gap and the material employed.[14] For a 5-μm TN cell, the response time is ~25 ms.

In summary, a simple method for fabricating LC-based microlens arrays has been demonstrated. Each microlens in the array exhibits hermaphroditic focusing properties. By switching the input light's polarization, we can change the focal length from positive to negative or vise versa. The means of fabrication is straightforward. Potential applications for image processing and flat-panel displays are foreseeable.

This research is supported by the Defense Advanced Research Project Agency Bio-Optic Synthetic Systems program under contract W911NF04C0048. S.-T. Wu's e-mail address is swu@mail.ucf.edu.

References

1. J. S. Patel and K. Rastani, Opt. Lett. **16,** 532 (1991).
2. N. A. Riza and M. C. DeJule, Opt. Lett. **19,** 1013 (1994).
3. T. Nose, S. Masuda, S. Sato, J. Li, L. C. Chien, and P. J. Bos, Opt. Lett. **22,** 351 (1997).
4. W. Klaus, M. Ide, Y. Hayano, S. Morokawa, and Y. Ariomoto, Proc. SPIE **3635,** 66 (1999).
5. L. G. Commander, S. E. Day, and D. R. Selviah, Opt. Commun. **177,** 157 (2000).
6. H. Ji, J. Kim, and S. Kumar, Opt. Lett. **28,** 1147 (2003).
7. Y. Choi, J. H. Park, J. H. Kim, and S. D. Lee, Opt. Mater. **21,** 643 (2002).
8. H. R. Stapert, S. del Valle, E. J. K. Verstegen, B. M. I. van der Zande, J. Lub, and S. Stallinga, Adv. Funct. Mater. **13,** 732 (2003).
9. H. Ren, Y. H. Fan, and S. T. Wu, Opt. Lett. **29,** 1608 (2004).
10. V. V. Presnyakov, K. E. Asatryan, T. V. Galstian, and A. Tork, Opt. Express **10,** 865 (2002), http://www.opticsexpress.org.
11. H. Ren, Y. H. Fan, S. Gauza, and S. T. Wu, Opt. Commun. **230,** 267 (2004).
12. S. Yanase, K. Ouchi, and S. Sato Jpn. J. Appl. Phys. **40,** 6514 (2001).
13. S. Sato, Jpn. J. Appl. Phys. **18,** 1679 (1979).
14. S. T. Wu and D. K. Yang, *Reflective Liquid Crystal Displays* (Wiley, New York, 2001).